

Supplementary Information

Histone chaperone exploits intrinsic disorder to switch acetylation specificity

Nataliya Danilenko¹, Lukas Lercher¹, John Kirkpatrick^{1,2}, Frank Gabel^{3,4}, Luca Codutti¹, Teresa Carlomagno^{1,2*}.

¹ Leibniz University Hannover, Centre for Biomolecular Drug Research, Schneiderberg 38, D-30167 Hannover, Germany.

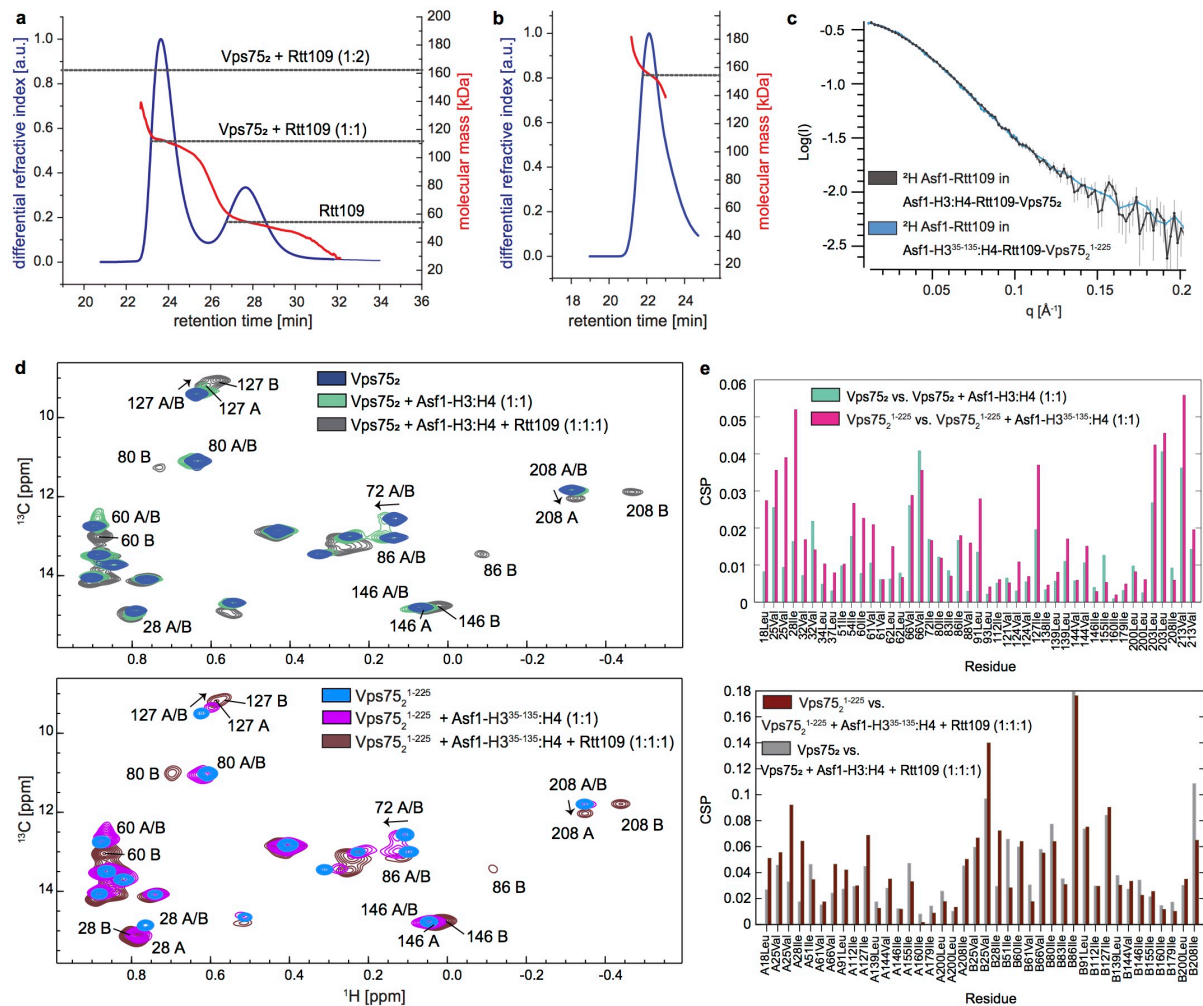
² Helmholtz Centre for Infection Research, Group of Structural Chemistry, Inhoffenstrasse 7, D-38124 Braunschweig, Germany.

³ University Grenoble Alpes, CEA, CNRS IBS, 71 avenue des Martyrs, F-38044 Grenoble, France.

⁴ Institut Laue-Langevin, 71 avenue des Martyrs, F-38042 Grenoble, France.

* Correspondence: teresa.carlomagno@oci.uni-hannover.de

Supplementary Figures



Supplementary Figure 1. Assembly of the *Sc* Asf1-H3:H4-Rtt109-Vps75₂ and Asf1-H3³⁵⁻¹³⁵:H4-Rtt109-Vps75₂¹⁻²²⁵ complexes. (a) SEC-MALS analysis of the Rtt109:Vps75 1:1 mixture at 50 μ M Rtt109. Red, molecular mass over the elution peaks; dashed grey lines, theoretical molecular masses of the corresponding complexes. Only one copy of Rtt109 binds the Vps75₂ homodimer. **(b)** SEC-MALS analysis of the *Sc* Asf1-H3:H4-Rtt109-Vps75₂ complex at 40 μ M confirms the stoichiometry. **(c)** Comparison of SANS curves of the Asf1-H3³⁵⁻¹³⁵:H4-Rtt109-Vps75₂¹⁻²²⁵ (blue) and Asf1-H3:H4-Rtt109-Vps75₂ (grey) complexes, assembled with ^2H -Rtt109/ ^2H -Asf1 in 42%:58% D₂O:H₂O buffer. The curves are scaled according to the concentration. **(d)** Overlay of ^1H - ^{13}C HMQC spectra of Vps75₂ in isolation and upon subsequent addition of Asf1-H3:H4 and Rtt109 (top); overlay of ^1H - ^{13}C HMQC spectra of Vps75₂¹⁻²²⁵ in isolation and upon subsequent addition of Asf1-H3³⁵⁻¹³⁵:H4 and Rtt109 (bottom). The CSPs of the Vps75 structured domains follow the same pattern in both Asf1-H3:H4-Rtt109-Vps75₂ and Asf1-H3³⁵⁻¹³⁵:H4-Rtt109-Vps75₂¹⁻²²⁵. **(e)** CSP analysis of the spectra in (d). Spectra were recorded on 60 μ M Vps75₂ in 50 mM sodium citrate pH 6.5, 150 mM NaCl, 5 mM BME at 850 MHz and 298 K. The titration of Vps75₂ used a D₂O-based buffer, while that for Vps75₂¹⁻²²⁵ used an H₂O-based buffer. The small differences in the exact values of the CSPs between the complex assembled with Vps75₂ and that assembled with Vps75₂¹⁻²²⁵ are due to the isotopic effects induced by the different solvents. Source data are provided as a Source Data file.

a

```

H3 Xen MARTKQTARKSTGGKAPRKQLATKAARKSAPATGGVKKPHRYRPGTVALR 50
H3 Xen# MARTKQTARKSTGGKAPRKQLATKAARKSAPATGGVKKPHRYRPGTVALR 50
H3 Sc MARTKQTARKSTGGKAPRKQLASKAARKSAPSTGGVKKPHRYKPGTVALR 50
*****:*****:*****:*****

H3 Xen EIRRYQKSTELLIRKLPFQRLVREIAQDFKTDLRFQSSAVMALQEASEAY 100
H3 Xen# EIRRYQKSTELLIRKLPFQRLVREIAQDFKTDLRFQSSAVMALQEASEAY 100
H3 Sc EIRRFQKSTELLIRKLPFQRLVREIAQDFKTDLRFQSSAIGALQESVEAY 100
****:*****:*****:*****:****:***

H3 Xen LVGLFEDTNLCAIHAKRVTIMPKDIQLARRIRGERA 136
H3 Xen# LVGLFEDTNLCAIHAKRVTIMPKDIQLARRIRGERA 136
H3 Sc LVSLFEDTNLAIAHAKRVTIQKDKILARRLRGERS 136
**:*****:*****:*****:****:****:****:

H4 Xen MSGRGKGGKGLGKGGAKRHRKVLRDNIQGITKPAIRRLARRGGVKRISGL 50
H4 Xen# MSGRGKGGKGLGKGGAKRHRKVLRDNIQGITKPAIRRLARRGGVKRISGL 50
H4 Sc MSGRGKGGKGLGKGGAKRHRKILRDNIQGITKPAIRRLARRGGVKRISGL 50
*****:*****:*****:*****:*****

H4 Xen IYEETRGVLKVFLENVIRDVITYTEHAKRKTVTAMDVVYALKRQGRRTLYG 100
H4 Xen# IYEETRGVLKVFLENVIRDVITYTEHAKRKTVTAMDVVYALKRQGRRTLYG 100
H4 Sc IYEEVRAVLKSFLESVIRDSVITYTEHAKRKTVTSLDVVYALKRQGRRTLYG 100
****:*** ***:****:*****:*****:*****:*****

H4 Xen FGG 103
H4 Xen# FGG 103
H4 Sc FGG 103
***

```

b

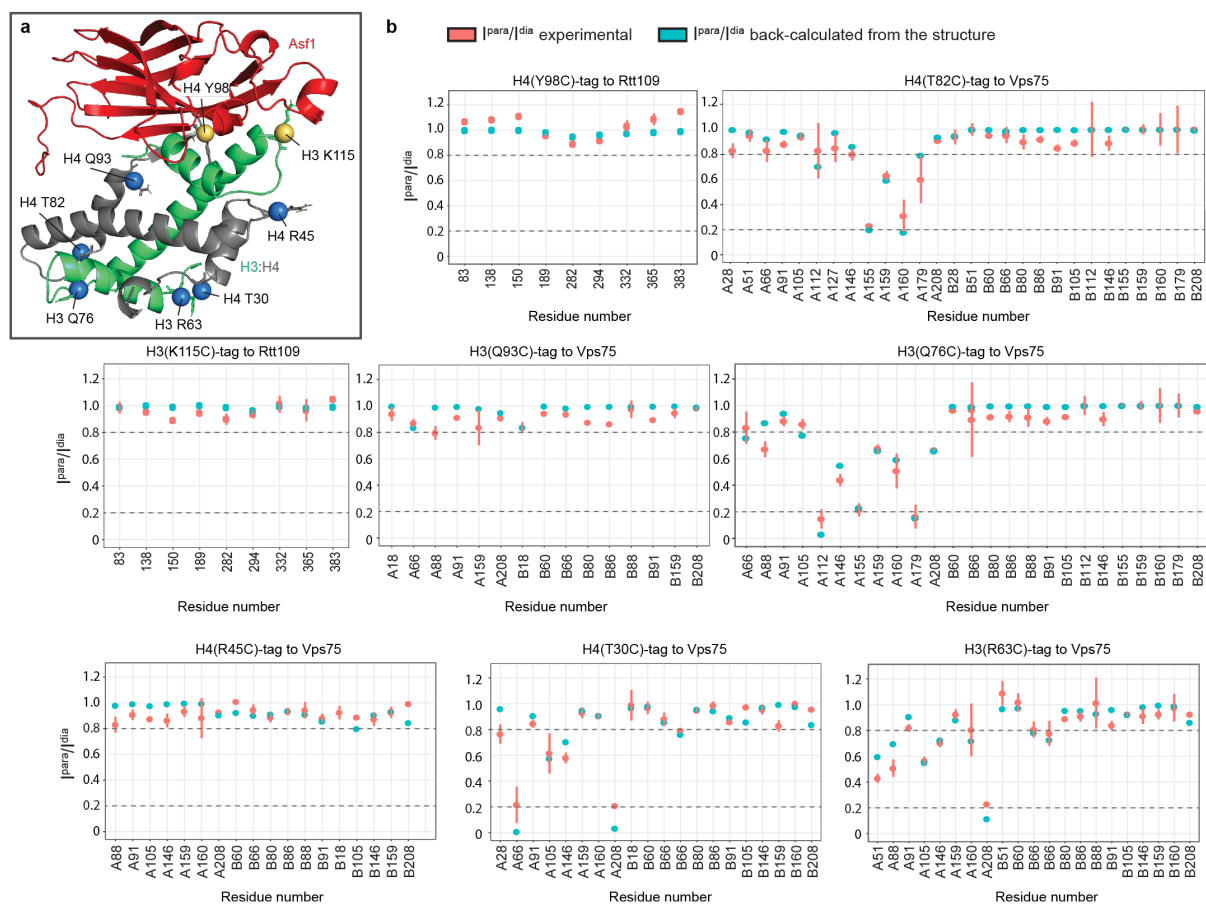
```

Sc AQRDL-EDEE-GESGLSADGDSE-DDDGSGLGEVDLPLSDEE----PSS-- 259
Sp AMTEEASDED---ESVDLEDEE-EEDEE--DEEG---DEEKQE-PPS-- 237
Ca ALSP-DEDDD---ANDEEDTTEGEE-----LDLSDDVVEE---PELPK 258
Cp ALSNESGEE---SEEEEDTSEGE-----LDLSDVVEEG-----K 265
Cg AQRDL-EDEE-DSSE--DNSS-E---PLDLEVESESESD----- 256
Kl AQRDVMDESD-GD-S---EDSDA-----PLDLDLEEVNDEGSDSKHLN 270

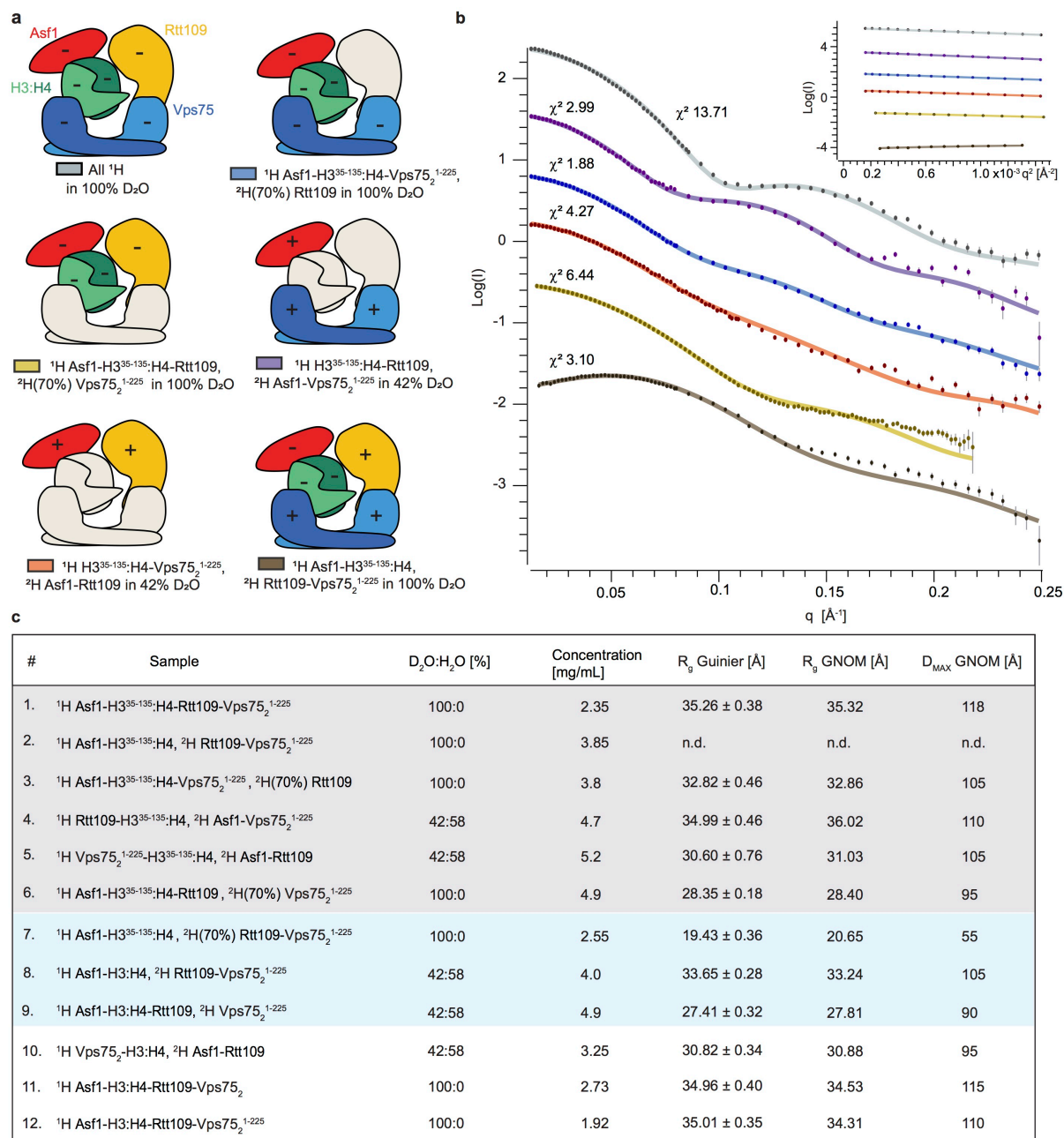
Sc -----KRRKV 264
Sp -----KSKKSN 244
Ca KRTLEEBENEHAT-KKSK 275
Cp KRTLGDIVDAPCEKVKQSSSV 288
Cg -----KRRKI 262
Kl -----KTKLQ 276

```

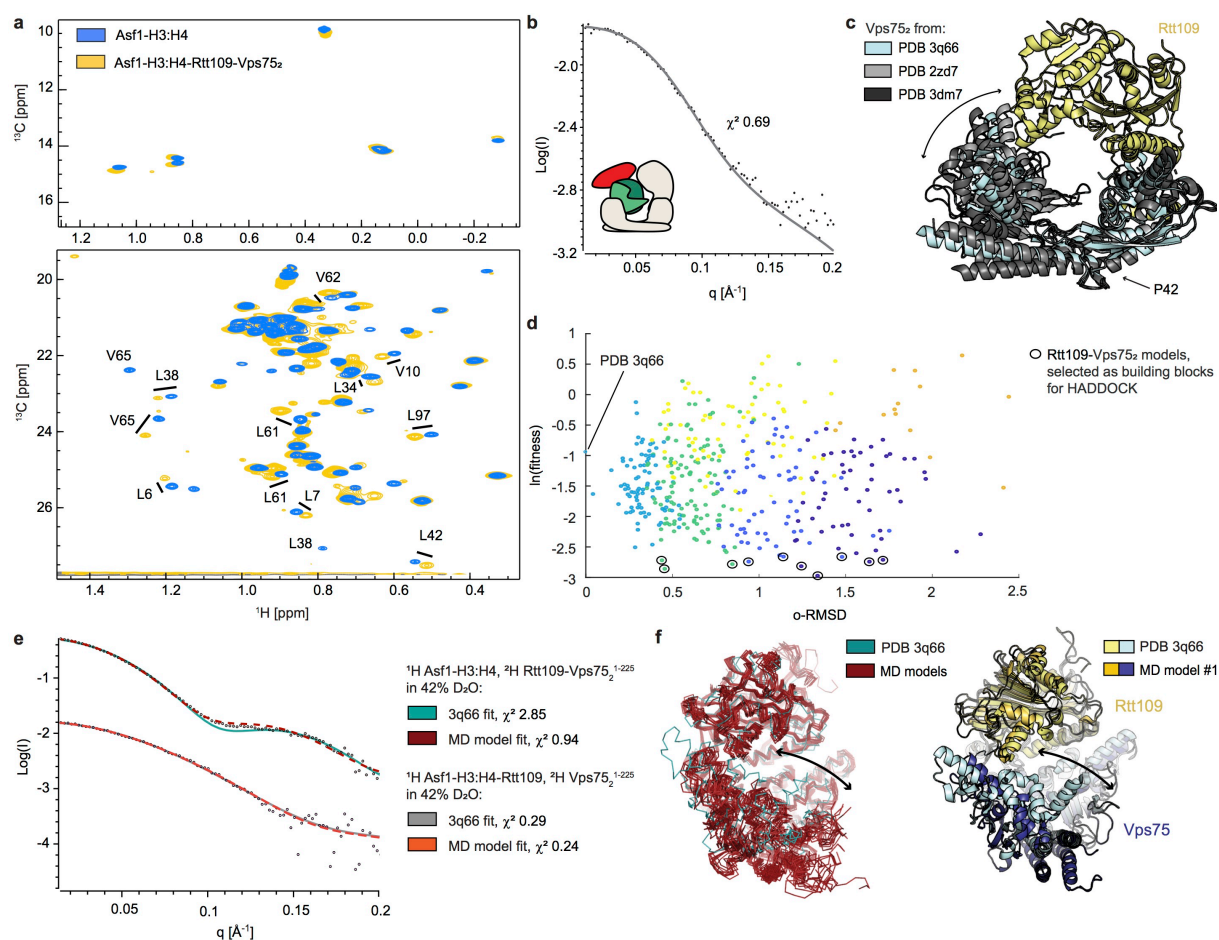
Supplementary Figure 2. (a) Sequence alignment of the histone sequences of *Xenopus laevis* (Xen), those used in this study (Xen #) and *Saccharomyces cerevisiae* (Sc). **(b)** Manual sequence alignment of the CTADs of Vps75 orthologs from organisms whose histone acetylation is dependent on Rtt109: *Saccharomyces cerevisiae* (Sc), *Schizosaccharomyces pombe* (Sp), *Candida albicans* (Ca), *Candida parapsilosis* (Cp), *Candida glabrata* (Cg), *Kluyveromyces lactis* (Kl).



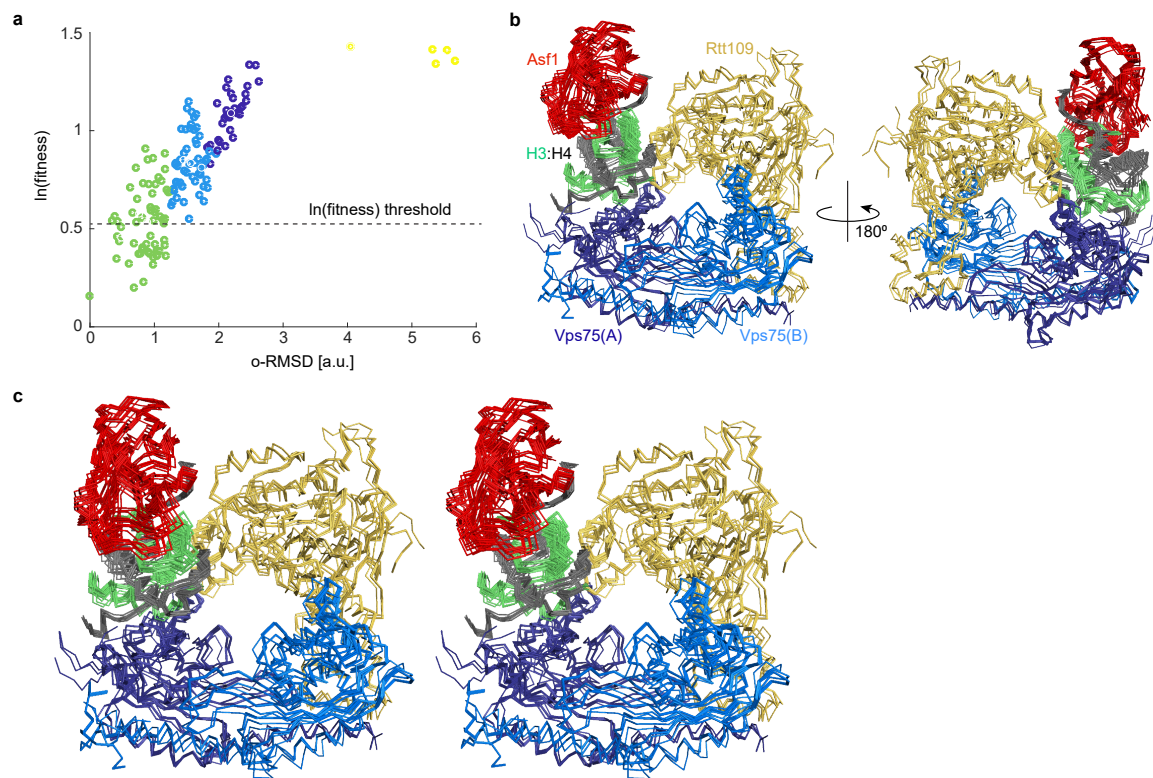
Supplementary Figure 3. Paramagnetic relaxation enhancements (PREs) (a) The positions of the paramagnetic tags are shown on the Asf1–H3:H4 subunit (PDB entry 2hue). Blue and yellow spheres indicate the tags used in PRE measurements of the ^1H - ^{13}C methyl groups of Vps75 and Rtt109, respectively. (b) Comparison of experimental (red) and back-calculated (light blue) ratios of peak intensities measured in the presence of the paramagnetic (I^{para}) or diamagnetic (I^{dia}) forms of the tags.



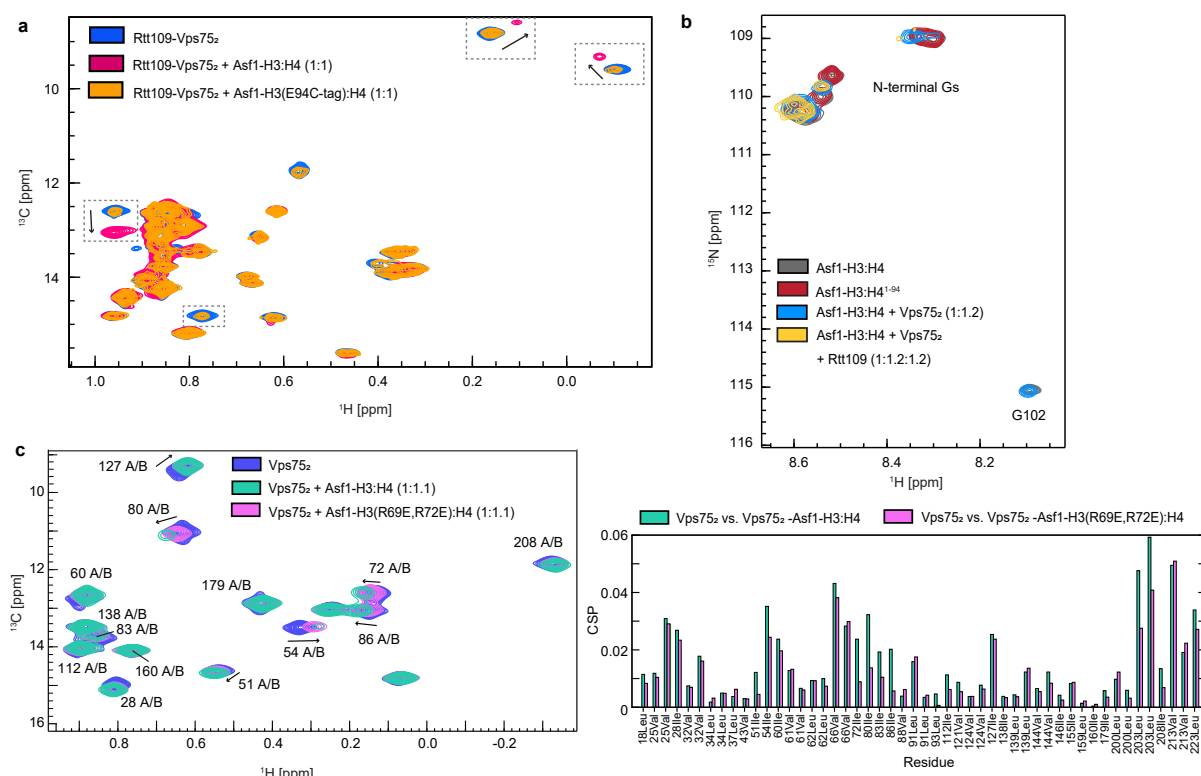
Supplementary Figure 4. Experimental SANS curves and their fits to those predicted from the Asf1-H3³⁵⁻¹³⁵:H4-Rtt109-Vps75₂¹⁻²²⁵ complex structure. (a) Schematic representation of the SANS complexes used in this study. The colored proteins contribute to the scattering-intensity with either positive (+) or negative (-) contrast, while the grey proteins are effectively invisible due to contrast-matching with the solvent. **(b)** Fits of the experimental curves with those predicted from the structure of Fig. 1. **(c)** Summary of the SANS measurements and the resulting structural parameters. Experiments 1–6 (grey) were used to select the final structures from M3 (Supplementary Fig. 6); experiments 7–9 (cyan) were used to select the structures of the Asf1-H3:H4 and Rtt109-Vps75₂ sub-complexes prior to M3 (Supplementary Fig. 5); experiment 10 (white) was not used in the structure calculations and was used for cross-validation; experiments 1, 11 and 12 were used to calculate the *ab initio* envelopes of Fig. 5.



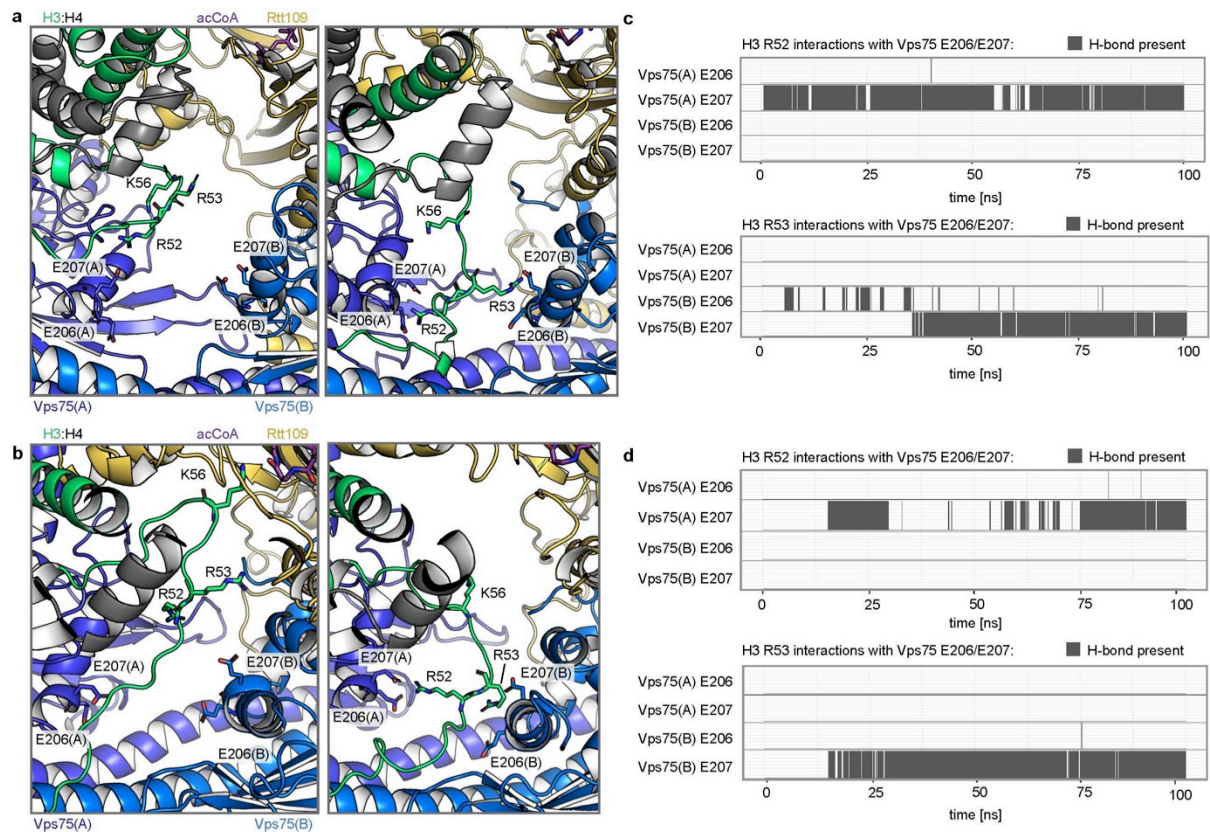
Supplementary Figure 5. (a, b) The Asf1–H3:H4 structure is conserved in complex with Rtt109–Vps75₂. **(a)** Overlay of ^1H - ^{13}C HMQC spectra of ILV methyl-labeled Asf1 as part of Asf1–H3:H4 and Asf1–H3:H4–Rtt109–Vps75₂ (top: Ile region; bottom: Leu/Val region). CS differences between the two spectra are observed only for the Asf1 surface containing amino acids ~35–75, which was previously shown to bind the Rtt109 C-terminal tail³⁷. Spectra were recorded on 50 μM Asf1 in 50 mM sodium citrate pH 6.5, 150 mM NaCl, 5 mM BME at 850 MHz and 298 K. **(b)** Overlay of the experimental SANS curve acquired for Asf1–H3^{35–135}:H4–Rtt109–Vps75₂ in 100% D₂O buffer, using ^1H -Asf1–H3^{35–135}:H4 and ^2H (70%)-Rtt109–Vps75, with the curve predicted from the structure of the Asf1–H3:H4–Rtt109–Vps75₂ complex generated using PDB entry 2hue as the Asf1–H3:H4 building block for M3. **(c–f). Selection of the Rtt109–Vps75₂ structures as building blocks for M3.** **(c)** Overlay of three crystal structures containing Vps75₂, demonstrating the variability of the hinge angle at residue P42. **(d)** Plot of the normalized χ^2 (see Methods for definition) versus o-RMSD (orientational root-mean-square deviation) to the structure of PDB entry 3q66 for the MD-generated conformers of the Rtt109–Vps75₂ complex. The o-RMSD was calculated for Vps75(A) relative to Rtt109. The normalized χ^2 was calculated using the SANS curves of Asf1–H3:H4–Rtt109–Vps75₂^{1–225}, acquired with ^2H -Vps75^{1–225} or ^2H -Rtt109 and ^2H -Vps75^{1–225} in 42%:58% D₂O:H₂O buffer. The conformers are clustered by o-RMSD and the clusters are shown in different colors. The ten structures with lowest normalized χ^2 , which contain representatives from the three best-scoring clusters, were selected as building blocks for M3. **(e)** Fits to the experimental SANS curves of the MD model with lowest normalized χ^2 and of the structure from PDB entry 3q66. **(f)** Structural variability of the ten selected conformers. The right panel displays the structural differences between the best MD model and PDB entry 3q66, which result in a more open cavity for substrate binding. The left panel shows that all selected models adopt the more open conformation.



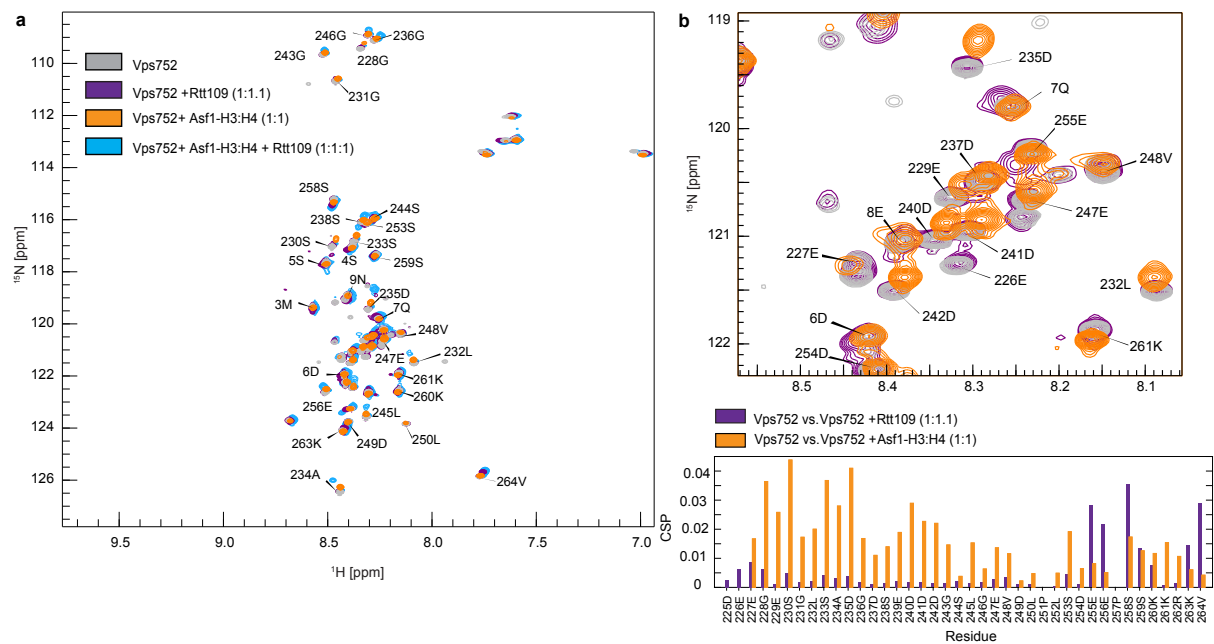
Supplementary Figure 6. Selection of the final ensemble. (a) Correlation between the structural similarity (orientational root-mean-square deviation, o-RMSD) of the conformations calculated by the M3 protocol and their agreement to the experimental SANS data, measured by the fitness parameter (Methods). The o-RMSD was calculated with respect to the structure with the best fitness; the structures were clustered by o-RMSD and each cluster is represented by one color. Members of the cluster that best fit the experimental data (green cluster) below the indicated threshold were selected as the final ensemble (33 structures). (b) Superposition of the ten best-fitness structures of the final ensemble. (c) Stereo view of the superposition of the ten best-fitness structures of the final ensemble.



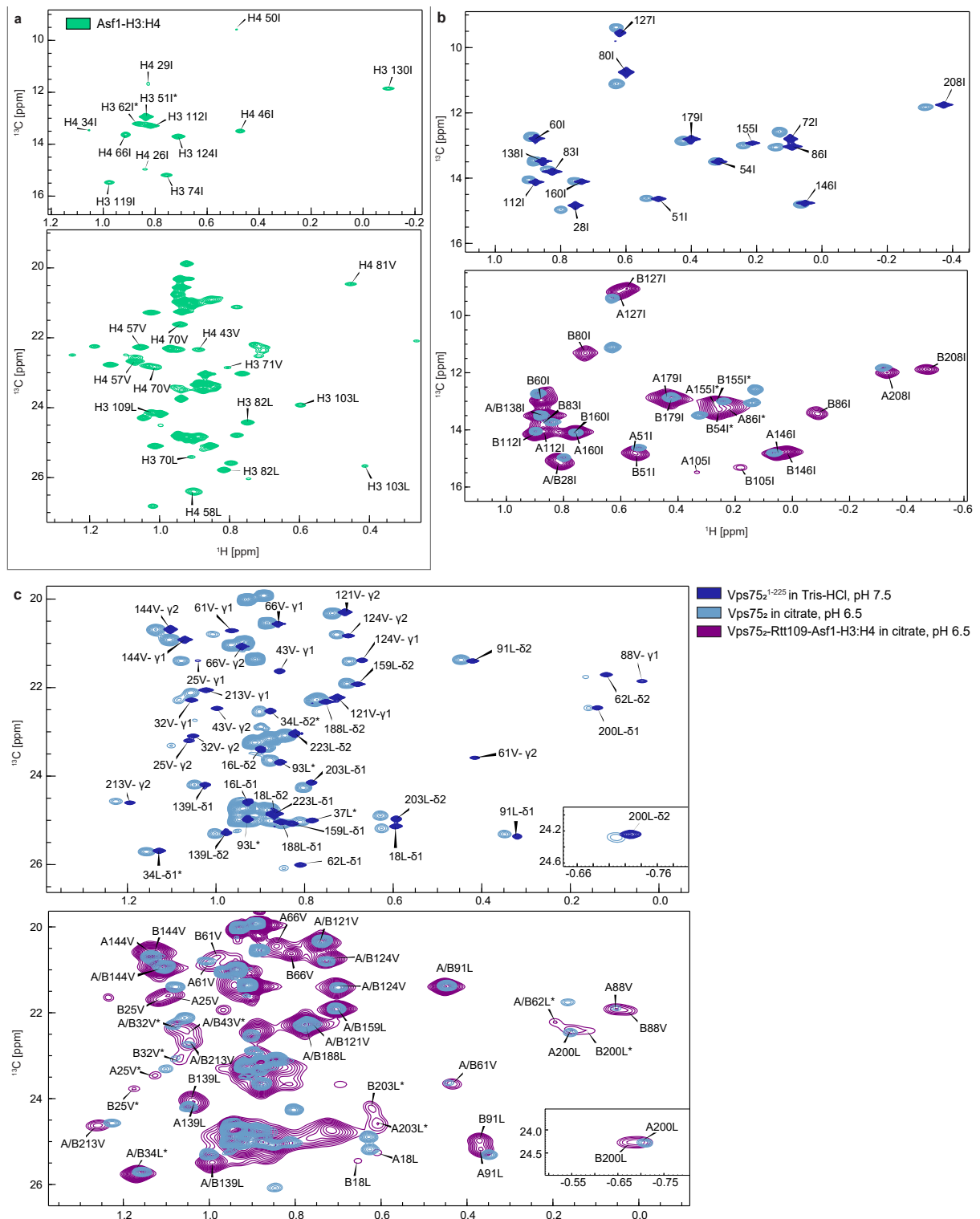
Supplementary Figure 7. Chemical shift perturbations at protein-protein interfaces. (a) ^1H - ^{13}C HMQC spectra of I-labeled Rtt109 as part of the Rtt109–Vps75₂ complex upon titration of Asf1–H3:H4 (pink) or Asf1–H3(E94C-tag):H4 (orange). “E94C-tag” denotes the presence of a paramagnetic tag coupled with the cysteine residue engineered at position 94 of H3. The peaks in the boxes display noticeable CSPs upon addition of wild-type Asf1–H3:H4, but not Asf1–H3(E94C-tag):H4. The spectra were recorded on ~65 μM Rtt109 in 50 mM sodium citrate pH 6.5, 150 mM NaCl, 5 mM BME at 850 MHz and 298 K. (b) ^1H - ^{15}N HSQC of ^{15}N -labeled H4 in the Asf1–H3:H4 complex upon titration of Vps75 (blue) and Rtt109 (yellow). Missing peaks of ^{15}N -labeled H4^{1–94} in Asf1–H3:H4^{1–94} (red) belong to the C-terminal region of H4 (H4^{95–102}). The spectra were recorded on 50 μM Asf1–H3:H4 in 50 mM sodium citrate pH 6.5, 150 mM NaCl, 5 mM BME at 600 MHz and 298 K. (c) ^1H - ^{13}C HMQC spectrum (left) and CSP plot (right) of ILV-labeled Vps75₂ in the presence of Asf1–H3:H4 or Asf1–H3(R69E,R72E):H4. The spectra were recorded on 60 μM Vps75 in 50 mM sodium citrate pH 6.5, 150 mM NaCl, 5 mM BME at 850 MHz and 298 K. Source data are provided as a Source Data file.



Supplementary Fig. 8. The acidic patch of Vps75 keeps K56 away from the Rtt109 catalytic pocket. **(a)** Right, final conformation of the MD simulation trajectory of Asf1–H3^{35–135}:H4–Rtt109–Vps75₂^{1–225}, starting from the structure (left) of Fig. 1 with the stretch H3^{35–59} built in an extended conformation, as in Fig. 3. **(b)** Right, final conformation of the MD simulation trajectory of Asf1–H3^{35–135}:H4–Rtt109–Vps75₂^{1–225}, starting from the structure (left) of Fig. 1 with the stretch H3^{35–59} modeled by placing K56 in the catalytic pocket of Rtt109. Both MD simulations in (a) and (b) resulted in the formation of stable H-bonds between H3-R52 and Vps75(A)-E207 as well as between H3-R53 and Vps75(B)-E207, which are incompatible with H3-K56 reaching the Rtt109 catalytic center. **(c)** Analysis of H-bonds present between H3-R52 or R53 and Vps75-E206 or E207 in the 100-ns MD simulations of Asf1–H3^{35–135}:H4–Rtt109–Vps75₂^{1–225} as in (a) and Fig. 3. **(d)** Analysis of H-bonds present between H3-R52 or R53 and Vps75-E206 or E207 in the 100-ns MD simulations of Asf1–H3^{35–135}:H4–Rtt109–Vps75₂^{1–225} as in (b).



Supplementary Fig. 9. (a) Overlay of ^1H - ^{15}N HSQC spectra of ^{15}N -labeled Vps75₂ in isolation (grey), in complex with Rtt109 (purple) and as part of either the Asf1–H3:H4–Vps75₂ (orange) or the Asf1–H3:H4–Rtt109–Vps75₂ (blue) complex. The chemical shift dispersion of the Vps75^{226–264} stretch remains very narrow indicating that the Vps75 CTAD stays disordered in all complexes. **(b)** Top, expansion of the overlay of ^1H - ^{15}N HSQC spectra of Vps75₂ in isolation (grey), in complex with Rtt109 (purple) and as part of Asf1–H3:H4–Vps75₂ (orange). Bottom, the CSP analysis demonstrates that the interaction between the Vps75₂ CTADs and Rtt109 affects different amino acids from those affected by the interaction with Asf1–H3:H4. Spectra were recorded on 50 μM Vps75 in 50 mM sodium citrate pH 5.5, 150 mM NaCl, 5 mM BME at 600 MHz and 298 K. Source data are provided as a Source Data file.



Supplementary Figure 11. Assignment of the methyl resonances of H3:H4 and Vps75. (a) ^1H - ^{13}C HMQC spectrum of ILV-labelled H3:H4 as part of the Asf1–H3:H4 complex (0.66 mM) in 20 mM Tris–HCl pH 7.5, 1 M NaCl, 1 mM Na-EDTA, 5 mM BME in 100% D₂O at 850 MHz and 298 K. (b, c) ^1H - ^{13}C HMQC spectra of ILV-labelled Vps75₂ (light blue) and Vps75₂ as part of the Asf1–H3:H4–Rtt109–Vps75₂ complex (purple) in 50 mM sodium citrate pH 6.5, 150 mM NaCl, 5 mM BME at 850 MHz and 298 K (b: Ile region, c: Leu/Val region with stereospecific assignment). The assignments are shown for the Vps75₂ and the Vps75₂ in the Asf1–H3:H4–Rtt109–Vps75₂ complex. In the latter spectrum, A and B indicate the Vps75(A) and Vps75(B) chains, respectively. The asterisk marks tentative assignments.